3D Eddy Current Computation in the Transverse Flux Induction Heating Equipment

Wolfgang Andree
ABB Industrietechnik AG IND/G, 44147 Dortmund, Germany

Dietmar Schulze and Zanming Wang
Subdepartment of Electroheat
Technical University of Ilmenau, 98684 Ilmenau, Germany

Abstract - **This paper describes a 3D computation of transverse flux inductors used for heating strip and thin slabs. The adopted mathematical model consists of a differential equation system for the steady-state eddy current problem in a configuration comprising a magnetic vector potential and a scalar potential and a Fourier's thermal conduction equation for moved media. The finite element method is applied in conjunction with the Galerkin method. The simplifications and boundary conditions required for an efficient solution are discussed. The discretization of the numerical model is set up with the aid of macroelements and includes upwards of 100 000 nodes for simple builds. The suitability of the numerical method developed for optimum design of transverse flux inductors is demonstrated by some results.**

I. Technological Problem

Induction heating or preheating of strip and thin slabs in a longitudinal flux in which the charge material is encircled by the inductor is subject to the condition that $d/\delta > 3$ applies if a good efficiency is to be accomplished. d is the thickness of the material and $\delta = 1/\sqrt{(\pi f \mu \kappa)}$ the equivalent depth of penetration with the frequency f, the permeability μ and the electric conductivity κ. This means, however, that an uneconomically high frequency > 10 kHz would have to be used for thin material. Thus, magnetic strip material up to about 0,8 mm thick, aluminium up to 4 mm thick and nonmagnetic steel up to 12 mm thick can be heated by induction in a longitudinal flux. These limits are lifted by the induction heating in the transverse flux.

In contrast to the longitudinal flux, the work piece is not encircled in the inductor. One each separate transverse flux inductor is usually arranged above and below the work piece. The magnetic flux chiefly passes vertically through the work piece. The eddy currents induced in the work piece close within the work piece surface, when a display of the primary currents flowing in the inductor is observed on the surface of the work piece.

Manuscript received November 1, 1993.

Initial numerical investigations into transverse flux inductors revealed that the inductor to strip width ratio has a considerable influence on the temperature distribution at the strip edge [1]. Long inductors protruding beyond the strip edge lead to edge overheating and a slight temperature valley forms in front of the edge. Short inductors result in a temperature decrease.

Joint application of both effects results in a multitude of feasible combinations going from extreme edge overheating to undercooling. With an optimised design, they can also result in almost homogenous temperature distribution across the strip width.

Using numerical modelling, parameter variation permits development of an optimum transverse flux inductor design. The primary objective of optimization is to accomplish a definite temperature distribution over the strip cross section downstream of the inductor outlet. The technological

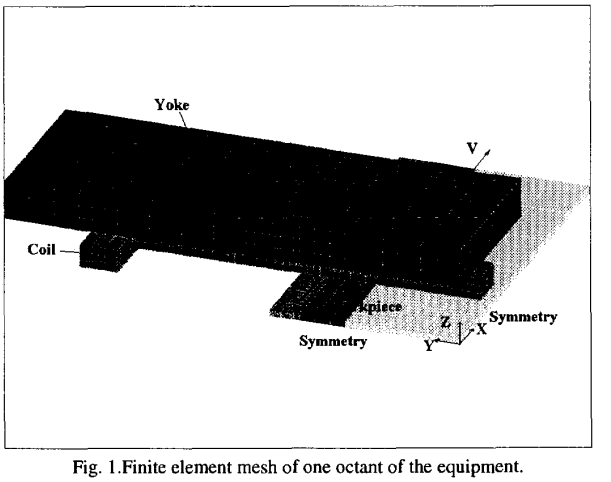

Fig. 1.Finite element mesh of one octant of the equipment. Half the strip width = 300 mm. Strip thickness = 15 mm Half the inductor length = 500 mm. Equivalent current penetration into strip = 30 mm. Half the inductor width = 125 mm. Coupling distance between inductor and strip = 20 mm.

problem definition specifies different temperature distributions at the inductor inlet as well as different work piece dimensions and materials. The objective of optimization can be influenced by the number of poles (inductors), their geometric shape (inductor, yoke) and the power source frequency.

II. Mathematical Model

The problem considered here is that of eddy currents at low angular frequencies ω. The displacement currents are neglected. Magnetic permeability μ and electric conductivity κ are assumed to be constant over longer periods of time (several cycles of the field-exciting voltages).

The mathematical model for this sinusoidal steady-state eddy current problem results from the Maxwell equations and is described by means of the complex magnetic vector potential $\underline{\vec{A}}$ and a complex scalar potential $\underline{\phi}$ [2].

$$\mathrm{rot}\,\frac{1}{\mu}\,\mathrm{rot}\,\underline{\vec{A}} + j\omega\kappa\left(\underline{\vec{A}} - \mathrm{grad}\,\underline{\phi}\right) = \kappa\,\vec{E}_S \qquad (1)$$

$\vec{E}_S$ is the electric field strength impressed by the power source. Moreover, the requirement of a solenoidal current density must be fulfilled.

$$\mathrm{div}\left(\underline{\vec{A}} - \mathrm{grad}\,\underline{\phi}\right) = 0 \qquad (2)$$

The scalar potential is, on the one hand, impressed in the solution area of the inductor by the applied external source voltage and the potential $\underline{\phi}$. On the other hand, and despite the numerically conditioned steadiness of the magnetic vector potential $\underline{\vec{A}}$, the requirement of a solenoidal current density

$$\underline{\vec{J}} = j\omega\kappa\left(\underline{\vec{A}} - \mathrm{grad}\,\underline{\phi}\right) + \kappa\,\underline{\vec{E}}_S \qquad (3)$$

is also met at interfaces.

The current density determines the heat source distribution.

$$p_V = J^2 / \kappa \qquad (4)$$

By the initial numerical investigations is shown that the introduction of the scalar potential $\underline{\phi}$ is indispensable, if the inductor protrudes beyond the strip edge.

The temperature field $\vartheta(x, y, z)$ is computed on the basis of the Fourier's thermal conduction equation.

$$\frac{\partial(c\rho\vartheta)}{\partial t} = \mathrm{div}\left(\lambda\,\mathrm{grad}\,\vartheta\right) + p_V - \bar{v}\,\mathrm{grad}\left(c\rho\vartheta\right) \qquad (5)$$

wherein λ is the thermal conductivity coefficient, c is the specific heat, ρ is the mass density and $\bar{v}$ is the strip velocity.

The two fields, the electromagnetic field and the temperature field which becomes steady-state at constant velocity, are coupled via the temperature dependence of the electric conductivity κ (x, y, z) and the magnetic permeability μ (x, y, z). This coupling is, however, relatively weak, because it is relatively easy to do with iterative functions for μ (x, y, z) and κ (x, y, z).

III. Numerical Model

The computation of the electromagnetic field by approximation is performed on the basis of the finite element method. The Galerkin method is applied to the differential equations (1) and (2), duly considering the boundary and symmetry conditions. The procedure is described in detail in [3].

For initial computations for orientation purposes, the reaction of the temperature field and the influence of the supply feeds (connecting leads) on the electromagnetic field are preferably neglected. Under these assumptions, three planes of symmetry can be defined. This reduces the solution area to 1/8 of the total volume.

In the x-z and the y-z planes of symmetry, the electric current density is oriented perpendicular to these planes. Hence for the tangential components of the magnetic vector potential $\underline{\vec{A}}$ and for the scalar potential $\underline{\phi}$:

$$\underline{\vec{A}}_{t1} = \underline{\vec{A}}_{t2} = 0 \qquad (6)$$

$$\underline{\phi} = 0 \qquad (7)$$

In the x-y plane of symmetry, the current density has no perpendicular component and

$$\underline{\vec{A}}_n = 0 \qquad (8)$$

$$d\,\underline{\phi} / d\,n = 0 \qquad (9)$$

In the present problem definition, the scalar potential in the electrically non-conductive field areas is practically insignificant because in the equations (1) and (3) it appears

always in conjunction with the electrical conductivity. The perpendicular component of the current density must be zero on the surface of electrically conducting areas, except for the impressed source current density. Hence the following is valid for:

$$j\omega\kappa\left(\vec{\underline{A}} - \operatorname{grad}\underline{\phi}\right)\cdot\vec{n} = 0 \tag{10}$$

As regards the magnetic vector potential, the present problem is an open boundary one because the vector potential disappears only in the infinite. With the aid of comparative computations, an enveloping surface can, however, be determined for which the condition

$$\vec{A} = \vec{0} \tag{11}$$

is valid with a known upper error limit.

For temperature field computation the solution area is restricted to the strip. But because of the mass-bound heat transfer, there is no y-z plane of symmetry. The heat sources in the newly added area can be obtained by reflection at the y-z plane or by separate computation for a corresponding temperature distribution. Thermal losses by convection and radiation on the strip surface are duly considered. On the side on which the strip enters the solution area, temperatures (e.g. ambient temperature) are given. On the exit side, however $\partial\vartheta/\partial x = 0$ (the x coordinate corresponds to the velocity direction) is indicated.

Dividing the solution areas into computation elements is necessary both for the 3D electromagnetic field and for the transient 3D temperature field. At the nodal points of these elements, the values of the vector potential $\vec{\underline{A}}$ and, additionally in the conductive areas, the values of the scalar potential $\underline{\phi}$ are computed. The coefficient matrix of the resulting algebraic equation system is positively definite, symmetric and sparse occupied. For the present practice relevant example, grids with up to 100,000 nodes or elements are required. The resulting very large matrices require specific storage types. For solving the equation system, the conjugate gradient method is used in the iterative solution process.

The computation of the temperature field of the moving strip is done on the basis of a particular grid. The heat source distribution, in the form of node values, is transferred to this grid (which can be not identical with the grid of the electromagnetic computation) by means of the shape functions. The influence of the velocity destroys the coefficient matrix symmetry of the equation system. A biconjugate gradient procedure or a relaxation procedure was therefore adopted as solution method. Test computations revealed that a better stability is accomplished by transient computation, wherefore the Cranck-Nickelson method was applied. Convergence problems at an increasing velocity were eliminated by adopting shorter time steps.

A semi-automatic process using what is termed macroelements is adopted for discretising the solution area. Macroelements are hexahedral, prismatic and tetrahedral elements which are automatically meshed and then assembled for overall discretization. Manual work is restricted to the definition of the macroelements. Grids with 100,000 elements can readily be set up. The macroelement concept does not fully exclude input errors. For this reason the completed discretisation is tested for meshing errors with a special program [4].

IV. Results

Fig. 1 shows the mesh of inductor (coil), yoke and strip. 11776 hexahedral elements with 13464 nodes resulted for the 1/8 of the overall computation domain, including the discretisation of the airfilled spaces; the latter is not shown

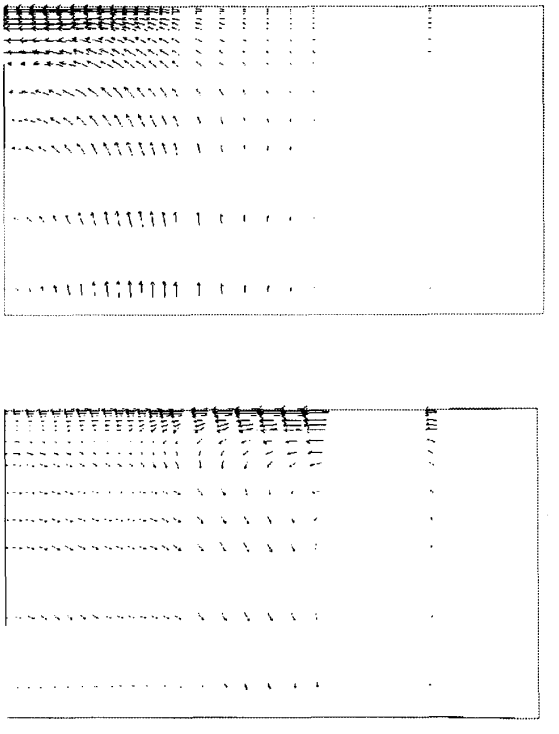

Fig. 2. Eddy current distribution on the strip surface: real part at the top, imaginary part at the bottom. N.B.: The measure of intensity is the arrow length, not the arrow density.

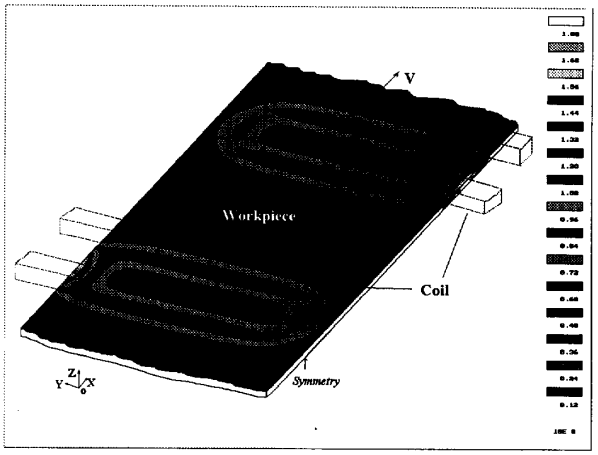

Fig. 3. Distribution of heat source density.

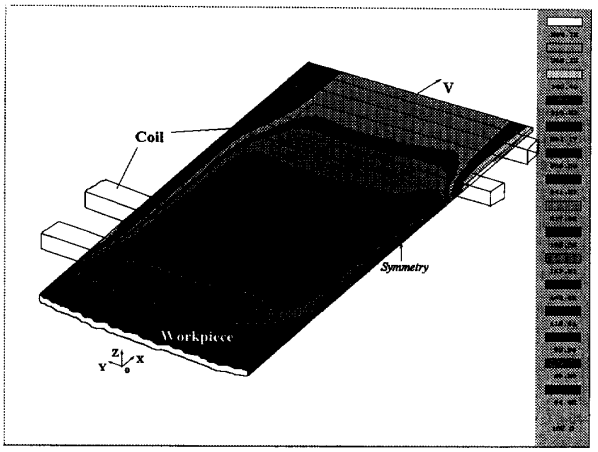

Fig. 5. Steady-state temperature distribution.

in the figure. The results presented below relate to this specific example which is one of many modifications [5].

The calculated eddy current distribution on the strip surface is illustrated in Fig. 2. Because the depth of current penetration is much greater than the strip width, a similar eddy current distribution will also occur in the deeper layers.

The density of heat source distribution according to eq. (4) is shown in Fig. 3.

If these heat sources are integrated along the x and the z coordinate, this will show the power density unit of length illustrated in Fig. 4 which would be proportional to the temperature rise if no thermal conduction and no surface heat losses were incurred.

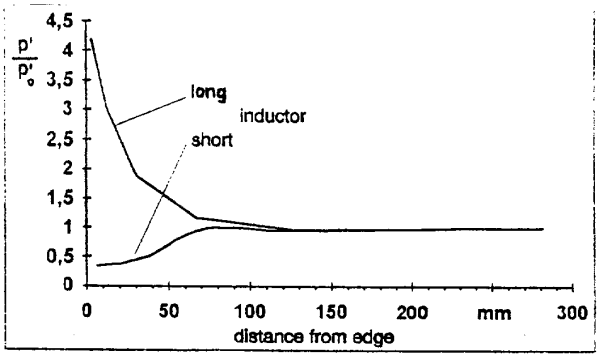

Fig. 4. Distribution of normalised integrated power density p' / p'_0 across the strip width

N.B.: The long inductor is according to Fig. 1 and the short inductor is approximately as wide as the strip.

The comparison of power density distributions for a long (computation example) and a short inductor indicates the possible combinations, configurations and geometries by which a desired final temperature distribution can be obtained.

Fig. 5 shows the temperature distribution resulting from the reflected heat sources distribution as per Fig. 3 in the steady-state situation. The computed results are confirmed by temperature measurements performed with an infrared camera.

REFERENCES

[1] W. Andree, H.-W. Mauwe, "Inductive Heating of thin sheet metal," *elektrowärme international*, vol. 50, No. 2, pp. B160-B164, August 1992.

[2] O. Biro, K. Preis, "On the use of the magnetic vector potential in the finite element analysis of three-dimensional eddy currents, " *IEEE Transaction on Magnetic*, vol. 25, No. 4, pp. 3145-3159, July 1989.

[3] Programmsystem PROMETHEUS des Fachgebietes Elektrowärme der Technischen Universität Ilmenau

[4] U. Lüdtke, "Zur numerischen Berechnung dreidimensionaler elektromagnetischer Felder," Dissertation, TH Ilmenau, 1990.

[5] W. Andree, D. Schulze, Z. Wang, "3D Wirbelstromberechnung für die induktive Querfelderwärmung, " Workshop Num. Feldberechnung in der Elektrowärme, Technical University of Ilmenau, Subdepartment of Electroheat, September 1993.